Proceedings of the XI DINAME, 28th February-4th March, 2005 - Ouro Preto - MG - Brazil
Edited by D.A. Rade and V. Steffen Jr.

IDENTIFICATION OF FLUTTER PARAMETERS FOR A WING MODEL

Carlos De Marqui Junior
demarqui@sc.usp.br

Daniela C. Rebolho
danielar@sc.usp.br

Eduardo Morgado Belo
belo@sc.usp.br

Flávio D. Marques
fmarques@sc.usp.br

Engineering School of Sao Carlos – University of Sao Paulo
Laboratory of Aeroelasticity, Flight Dynamics and Control
Av. Trabalhador Sancarlense 400, 13566- 590, Sao Carlos, SP, Brazil.

Abstract. *A flexible mounting system has been developed for flutter tests with rigid wings in wind tunnels. This flexible mounting provides a well-defined two-degree-of-freedom system on which rigid wings can encounter classical flutter. A classical two-degree-of-freedom flutter is a combination of structural bending and torsion vibration modes. Active control schemes for flutter suppression can be tested using this experimental setup using a trailing edge flap as actuator. Before the development of control schemes some tests can be performed to identify flutter parameters. Initially, some wind tunnel tests are performed to verify the critical flutter velocity and critical frequency. After this, some tests are performed to characterize the flutter phenomenon. Frequency response functions are obtained for the range of velocities below the critical one, showing the evolution of pitch and plunge modes and the coupling tendencyof these modes with increasing velocity. The pitch and plunge data of these tests are also acquired in time domain and an Extended Eigensystem Realization Algorithm (EERA) is used to identify flutter parameters with increasing velocity. These results are demonstrated as an identified V-g plot, showing the evolution of frequency and damping of the modes involved in flutter with increasing velocity and flutter achievement.*

Keywords*: Identification, Flutter, EERA, Aeroservoelasticity.*

1. Introduction

Aeroelastic effects are a result of the interaction of elastic and inertial structural forces. If structures were to remain perfectly rigid when exposed to an airstream, aeroelastic problems would not exist. However, aircraft structures are flexible and this characteristic is fundamentally responsible for some types of aeroelastic phenomena. When elastic bodies are exposed to airstream, structural deformations induce additional aerodynamic forces and these forces produce additional structural deformations, which again will induce greater aerodynamic forces. This interaction may lead to aeroelastic instabilities, like flutter for example (Försching, 1979). After World War II the increase in flight speed and structural modifications made aeroelastic problems more significant. The changes and historical evolution of aeroelasticity through out the history are described in Ashley (1970), Collar (1959), Garrick and Reed (1981), and Garrick (1976).

Flutter is one of the most representative topics of aeroelasticity. Flutter is a complex phenomenon where, in classical terms, structural modes are coupled and excited by aerodynamic loads. In a more formal way, flutter is the condition when an aircraft component exhibits a self-sustained oscillatory behaviour at speeds higher than the critical one (Wright, 1991). The critical flutter speed is the frontier between aeroelastic stability and instability. In general, flutter occurs on lifting surfaces submitted to large aerodynamic loads, such as wings and tails.

Considering the destructive behaviour of flutter, wind tunnel tests are an important way to the development of preliminary experimental aeroelastic tests. These tests may be conducted with flexible wing models like (Mukhopadhyay, 1995) or with rigid wing models associated with flexible mounting systems like in (Ko *et al*., 1997 and Waszak, 1998). The first alternative is a more realistic representation of a flutter problem, but considering the integrity of the wind tunnel and equipments the second solution is a safer way to the implementation of flutter tests. So, considering these facts and the difficulties involved, the second alternative was considered the most prudent one.

A flexible mounting system was designed to permit motions in two-degree-of-freedom, that is, pitch and plunge. During the design period, a Finite Element Model (FEM) of the mounting system was developed and its dimensions and dynamical characteristics were determined. These analytical characteristics were tested with an aeroelastic model in order to verify critical flutter velocity. The dimensions of the FEM model, and consequently its dynamical characteristics, were modified until the aeroelastic behaviour of the system was adjusted to the available wind tunnel.

The dynamical properties of the physical system were then confirmed with an Experimental Modal Analysis and then the wind tunnel tests were performed (De Marqui Jr *et al*., 2004).

Flutter characterization and an identification process of some flutter parameters were performed using the data acquired during the wind tunnel tests. The flutter characterization was verified with Frequency Response Functions obtained for the range of velocities below the critical one. These frequency responses could show the evolution of pitch and plunge modes with increasing velocity and the coupling tendency of these modes near the critical velocity.

During the same tests, time domain aeroelastic responses were acquired for the range of velocities below the critical one. Using these time domain responses the main objective of this work could be achieved: the identification of some flutter parameters (frequency and damping) using the identification method known as extended Eigensystem Realization Algorithm - EERA. The EERA method, a modified form of a batch algorithm method, calculates the modal parameters by manipulating both input and output time histories (obtained during the wind tunnel tests), being necessary the knowledge of the excitation data. The block Hankel matrices are built directly from the system input and output time history database.

The development of subspace identification methods was motivated by difficulties in estimating modal parameters for multiple-input multiple-output vibratory systems (Tasker *et al.*, 1998). During the last few years these methods have attracted attention in the field of system identification because they are essentially non-iterative (therefore, no convergence problems arise), fast and numerically robust (since they are only based on numerically stable techniques of linear algebra) (Favoreel *et al*., 1999). These methods accomplish substantial filtering of the data using eigenvalue or singular value decomposition and are particularly effective when there are closely spaced modes. In essence, the data are separated into orthogonal signal and null subspaces, either of which may be used to estimate the modal parameters (Tasker *et al.*, 1998).

2. Physical Model

The physical model used was a rigid wing with a NACA 0012 airfoil section associated with a flexible mounting system. The flexible mounting system provides a well-defined two-degree-of-freedom dynamic system on which rigid wing will encounter classical flutter. A side and perspective view of the flutter mounting system are presented in Fig. 1. The flutter mounting system consists of a moving plate supported by a system of four circular rods and a centered flat-plate strut, similar to the system developed in Dansberry *et al*. (1993).

The rods and the flat-plate provide the elastic constraints and the rigid wing model fixed in the moving plate will oscillate in a two-degree-of-freedom mode, that is, pitch and plunge, when flutter is encountered. The rods, flat-plate and moving plate are made of steel and all connections are fixed-fixed end. The wing model is made of aluminum and the trailing edge flap is made of ABS resin. Their dimensions are: rods 0.0055 *m* in diameter; moving plate is 0.6×0.3 *m*; flat-plate is 0.7×0.1×0.002 *m* and wing model has 0.8×0.45 *m*.

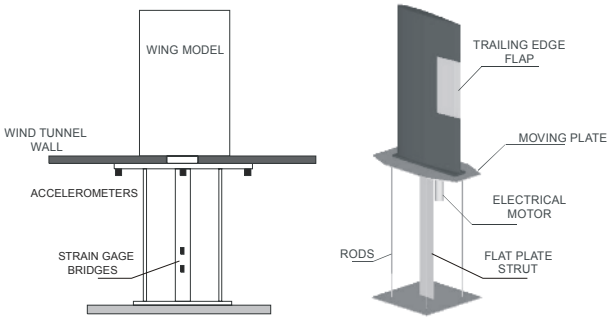

Figure 1. Side and perspective views of the flutter mounting system.

The wind-off characteristics of the flutter mounting system are strongly influenced by the dimensions of the flat-plate strut, the rods and the mass of the moving plate and wing model. Modifications in the length and cross section of the flat plate strut and rods modify the frequencies and mode shapes of the flexible mounting system. Weights can be added to decouple the pitch and plunge modes by moving the centre of gravity of the flexible mounting and wing model to the system elastic axis. The system elastic axis is located in the vertical centreline of the flat plate strut and centre of the moving plate. The four rods also assure a parallel pitch and plunge displacement relative to the wind tunnel wall.

To design the flexible system, a Finite Element Model is generated. This model is employed as a tool for the flexible flutter mounting system design. The cantilever boundary condition is adopted for the flexible mounting system at the rods and flat plate strut. Of course, this is an ideal condition adopted for the simulations and it is not strictly verified in the physical system.

An Experimental Modal Analysis is performed to verify the natural frequencies and modes prior to any wind tunnel flutter test. In this test, frequencies below 25 *Hz* are investigated and the wing control surface is locked. The measurement points are located at the flat-plate strut, because it provides the elastic constraints to the system, being the wing model considered rigid. The Eigensystem Realization Algorithm (ERA) modified by Tsunaki (1999) is employed

to identify the modes shapes and frequencies from the experimental data. The most significant natural frequencies are listed in Tab. 1. Rods and chordwise modes are not investigated in this Modal analysis.

Table 1 shows first bending and first torsion modes well defined and also show the third mode higher than those. Theoretically, this condition assures a two-degree-of-freedom system during the wind tunnel tests and also that higher modes will not be significantly excited (Dansberry *et al*., 1993). Details on the flexible mounting system design procedure and more results can be found in De Marqui Jr *et al*. (2004).

The above analysis takes into account only the structural aspects of the flutter problem. Obviously the interaction of these characteristics with the aerodynamic ones has to be considered in the flutter analysis. Aerodynamic forces and moments, lift and pitch moment in the case of this study, will be exciting the modes involved in the classical bending-torsion flutter. As consequence, the elastic characteristics of the structure and the resulting aerodynamic restoring loads (responsible for aerodynamic damping when no mechanical friction is assumed and caused by the upwash induced by the wake vortices) will be reacting and dissipating energy to the airstream. When the critical speed is achieved, the aerodynamic damping vanishes because the aerodynamic restoring forces lose their dissipative characteristics and the self-sustained oscillatory behaviour is verified. This procedure is given in standard text (Fung, 1993).

Table 1. Natural frequencies of the flexible mounting system and wing model identified with ERA.

Mode	Frequency (*Hz*)	Description
1	1.2	First bending (plunge)
2	2.4	First torsion (pitch)
3	11.7	Second bending

The experimental system, wing associated with the mounting system, is instrumented with two strain gauges and three accelerometers, as can be seen in Fig 1. The strain gauges are positioned on the flat plate strut and they measure pitch and plunge displacements. The capacitive accelerometers measure pitch and plunge motions and they are positioned on the system elastic axis (plunge) and on the trailing edge and leading edge areas (pitch). The trailing edge flap ranges from 37.5 % to 62.5 % of the wingspan and covering 35 % of the chord. A brushless dc motor associated with a servo amplifier is used to control this control surface through connecting shafts. The motor position control is based on a proportional-integral-derivative (PID) controller. The motor position is the feedback signal and is measured with its encoder.

3. Identification Method - EERA

Any linear time-invariant dynamic system with n degree-of-freedom can be modeled by the following discrete time state space equations:

$$\begin{cases} \{x(k+1)\} = [A_d]\{x(k)\} + [B_d]\{u(k)\} \\ \{y(k)\} = [C_d]\{x(k)\} + [D_d]\{u(k)\} \end{cases} \tag{1}$$

where $\{x(k)\}$ is the $2n$ – dimensional state vector at the k th sample instant, $\{u(k)\}$ is the r - dimensional input vector, being r the number of external excitations, $\{y(k)\}$ is the m - dimensional response vector, being m the number of output (response of the system), $[A_d]$ is the $2n \times 2n$ system matrix, $[B_d]$ is the $2n \times r$ input matrix, $[C_d]$ is the $m \times 2n$ output matrix and $[D_d]$ is the $m \times r$ direct transmission matrix.

Defining the block Hankel matrices of inputs and outputs, constructed from the direct input-output data:

$$[U] = \begin{bmatrix} \{u(0)\} & \{u(1)\} & \cdots & \{u(N-1)\} \\ \{u(1)\} & \{u(2)\} & \cdots & \{u(N)\} \\ \vdots & \vdots & \vdots & \vdots \\ \{u(M-2)\} & \{u(M-1)\} & \cdots & \{u(M+N-3)\} \\ \{u(M-1)\} & \{u(M)\} & \cdots & \{u(M+N-2)\} \end{bmatrix}_{rM \times N} \quad [Y] = \begin{bmatrix} \{y(0)\} & \{y(1)\} & \cdots & \{y(N-1)\} \\ \{y(1)\} & \{y(2)\} & \cdots & \{y(N)\} \\ \vdots & \vdots & \vdots & \vdots \\ \{y(M-2)\} & \{y(M-1)\} & \cdots & \{y(M+N-3)\} \\ \{y(M-1)\} & \{y(M)\} & \cdots & \{y(M+N-2)\} \end{bmatrix}_{mM \times N} \tag{2}$$

Considering that $[\Gamma]$ is an extended observability matrix, $[X]$ is a matrix of the state sequence and $[G]$ is a block Toeplitz matrix of Markov Parameters or impulse response, i.e.,

$$[\Gamma]=\begin{bmatrix}[C_d]\\ [C_d][A_d]\\ [C_d][A_d]^2\\ \vdots\\ [C_d][A_d]^{M-1}\end{bmatrix}_{mM\times 2n} \qquad [X_d]=[\{x(1)\}\ \ \{x(2)\}\ \ \cdots\ \ \{x(N)\}]_{2n\times N}$$

$$[G]=\begin{bmatrix}[D_d] & [0] & \cdots & [0]\\ [C_d][B_d] & [D_d] & \cdots & [0]\\ [C_d][A_d][B_d] & [C_d][B_d] & \cdots & [0]\\ \vdots & \vdots & \vdots & \vdots\\ [C_d][A_d]^{M-2}[B_d] & [C_d][A_d]^{M-3}[B_d] & \cdots & [D_d]\end{bmatrix}_{mM\times rM} \tag{3}$$

it can be verified that (Verhaegen and Dewilde, 1992)

$$[Y]=[\Gamma][X]+[G][U] \tag{4}$$

By definition, the orthogonal matrix U can be written as:

$$[U]^{\perp}=[I]-[U]^t\left([U][U]^t\right)^{-1}[U] \tag{5}$$

Using Eq. (4) and Eq. (5), results in:

$$[Y][U]^{\perp}=[\Gamma][X][U]^{\perp} \tag{6}$$

Using the singular value decomposition,

$$[Y][U]^{\perp}=[[R_{2n}]\ \ [R_0]]\begin{bmatrix}[\Sigma_{2n}] & [0]\\ [0] & [0]\end{bmatrix}\begin{bmatrix}[S_{2n}]^t\\ [S_0]^t\end{bmatrix}=[R_{2n}][\Sigma_{2n}][S_{2n}]^t \tag{7}$$

where $[R_{2n}]$ is the $mM\times mM$ matrix of the left singular vectors that span the principal or singular subspace, $[\mathbf{\Sigma}_{2n}]$, $mM\times N$ - dimensional, are the corresponding singular values and $[S_{2n}]$, $N\times N$ - dimensional, are the corresponding right singular vectors.

Considering $[Y_s]$ a shifted form of the block Hankel matrix of the output,

$$[Y_s]=\begin{bmatrix}\{y(1)\} & \{y(2)\} & \cdots & \{y(N)\}\\ \{y(2)\} & \{y(3)\} & \cdots & \{y(N+1)\}\\ \vdots & \vdots & \vdots & \vdots\\ \{y(M-1)\} & \{y(M)\} & \cdots & \{y(M+N-2)\}\\ \{y(M)\} & \{y(M+1)\} & \cdots & \{y(M+N-1)\}\end{bmatrix}_{mM\times N} \tag{8}$$

in a similar way to Eq. (4), one obtains

$$[Y_s]=[\mathbf{\Gamma}_s][X]+[G_s][U] \tag{9}$$

where

$$[\Gamma_s]=\begin{bmatrix}[C_d][A_d]\\ [C_d][A_d]^2\\ [C_d][A_d]^3\\ \vdots\\ [C_d][A_d]^M\end{bmatrix}_{mM\times 2n} \quad \text{and} \quad [G_s]=\begin{bmatrix}[C_d][B_d] & [D_d] & \cdots & [0]\\ [C_d][A_d][B_d] & [C_d][B_d] & \cdots & [0]\\ [C_d][A_d]^2[B_d] & [C_d][A_d][B_d] & \cdots & [0]\\ \vdots & \vdots & \vdots & \vdots\\ [C_d][A_d]^{M-1}[B_d] & [C_d][A_d]^{M-2}[B_d] & \cdots & [D_d]\end{bmatrix}_{mM\times rM} \tag{10}$$

which are shifted versions of the matrices of Eq. (3).

It is, then, possible to obtain two matrices, that is,

$$[Y][U]^{\perp} = [\Gamma][X][U]^{\perp}$$
$$[Y_s][U]^{\perp} = [\Gamma_s][X][U]^{\perp} = [\Gamma][A][X][U]^{\perp} \tag{11}$$

A transition matrix, $[T]$, may be estimated by solving

$$[T][Y][U]^{\perp} = [Y_s][U]^{\perp} \tag{12}$$

Thus

$$[\Gamma] = [Y_s][U]^{\perp}\left([Y][U]^{\perp}\right)^{\dagger} = [\Gamma][A_d][X][U]^{\perp}\left([X][U]^{\perp}\right)^{\dagger}[\Gamma]^{\dagger} \Rightarrow [A_d] = [\Gamma]^{\dagger}[Y_s][U]^{\perp}\left([Y][U]^{\perp}\right)^{\dagger}[\Gamma] \tag{13}$$

For the Eq. (7), a valid representation of the extended observability matrix is,

$$[\Gamma] = [R_{2n}][\Sigma_{2n}]^{1/2} \tag{14}$$

In this way, for the Eq. (14), the $[A_d]$ system matrix is given by,

$$[A_d] = [\Gamma]^{\dagger}[Y_s][U]^{\perp}([Y][U]^{\perp})^{\dagger}[\Gamma] = [\Sigma_{2n}]^{-1/2}[R_{2n}]^{t}[Y_s][U]^{\perp}[S_{2n}][\Sigma_{2n}]^{-1/2} \tag{15}$$

and $[C_d]$ is estimated as the first block partition of the estimated $[\boldsymbol{\Gamma}]$. Natural frequencies and damping ratio are obtained from the eigenvalues of $[A_d]$.

The above expression differs from the ERA expression only by the presence of the input term. When the responses are due to impulsive inputs, the expression is identical to the expressions observed in ERA.

4. Experimental Flutter Verification

The experimental setup is based on a dSPACE system for data acquisition and trailing edge flap control. This system has a DS1103 processor board with a 400*Mhz* Power PC 604e processor and 128 *MB* of RAM. The system also allows simultaneous I/O operations with the 4 AD units multiplexed in 4 channels each (4 *ms* maximum sampling time), 8 DA channels and 6 incremental encoder interfaces.

The sampling frequency for acquisition and control surface actuation is set to 1000 Hz. A brushless dc motor drives the trailing edge flap and a PID controller is set to control the motor position. The motor position is given by its encoder and acquired on the dSPACE board. The PID controller was adjusted and tested previously at several wind tunnel velocities.

The first wind tunnel test was performed to verify the critical flutter velocity. The wind tunnel velocity was gradually increased and the pitch and plunge signals were measured using the dSPACE system. Flutter was observed at the critical flow velocity of 25 *m/s*, when the oscillatory behaviour was measured. Figure 2 presents, respectively, the pitch and plunge displacement measured during these experiments.

One of the characteristics of the flutter phenomenon is the coupling of the modes, pitch and plunge in the case of this study. This condition is verified in Fig. 3, where the time domain signals presented in Fig. 2 are presented in terms of their frequency content.

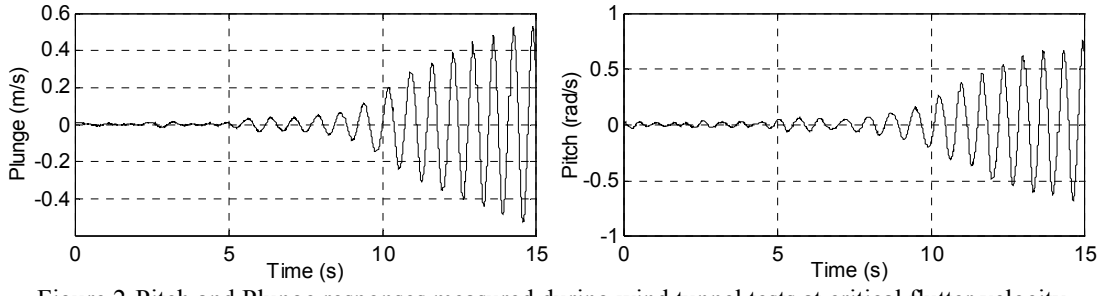

Figure.2 Pitch and Plunge responses measured during wind tunnel tests at critical flutter velocity.

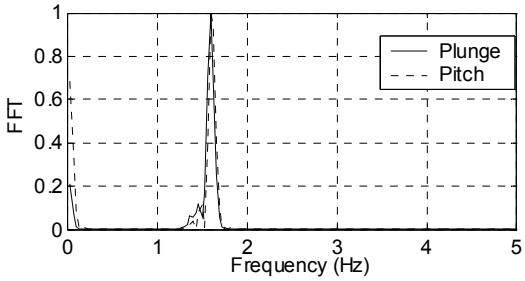

Figure.3 Frequency domain representation of Pitch and Plunge responses obtained during wind tunnel tests at critical flutter velocity.

This test shows the behaviour of the system only at the critical velocity. But some dynamical characteristics change with increasing wind tunnel flow velocity. In order to verify these changes other tests were performed. Basically, frequency response functions were obtained in several velocities showing the evolution of first bending and torsion modes with increasing velocity. The input signal considered during these tests is the trailing edge position and the output signal is the acceleration measured in the trailing edge region of the wing.

A B&K dual channel digital spectrum analyzer type 2032 was employed to obtain the frequency responses. These responses are obtained from the wind tunnel off condition up to velocities as near as possible of the critical one. The signal input is a white noise generated in the dSPACE system and sent to the trailing edge flap. This signal and the acceleration are processed in the spectrum analyzer. This procedure is repeated for all intermediate test velocities.

In Fig. 4, one can verify the evolution of the modes with increasing wind tunnel velocity. The frequency response obtained at zero velocity presents peaks relative to first bending and torsion modes well-defined and the same natural frequencies obtained during the EMA, as expected. In the last frequency response, measured near to the critical velocity, one can verify the tendency of coupling between the modes involved in flutter. This coupling occurs at frequency about 1.6 *Hz*, confirming the result observed in Fig. 3.

In the frequency responses obtained in intermediate velocities, the variations in pitch and plunge frequencies can be observed. Also, it is clear that the peaks of pitch and plunge modes are not so sharp as the peaks of the frequency response at zero velocity. This fact can be seen as the effect of fluid structure interaction on damping increasing. This tendency is expected until velocities near the critical one, when the damping is expected to vanish and flutter occurs.

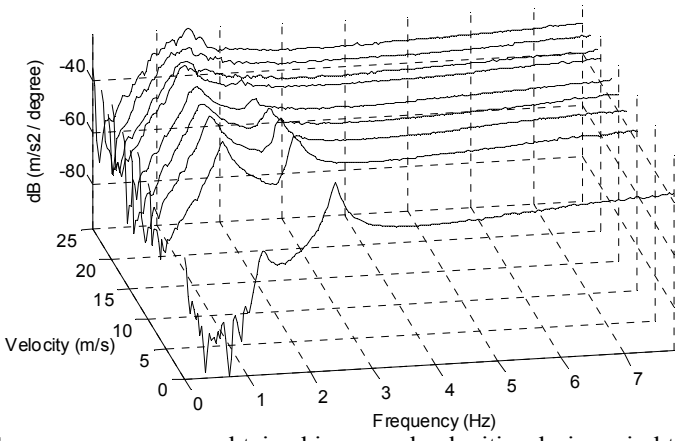

Figure.4 Frequency responses obtained in several velocities during wind tunnel tests.

5. Identification Results

The extended Eigensystem Realization Algorithm (EERA) was employed to quantify the variation of frequencies and damping values relative to the modes involved in flutter with wind tunnel increasing velocity.

The data used in the identification process were acquired during the tests performed to obtain the frequency response function previously described. Simultaneously to the frequency domain tests, the input signal (trailing edge flap position) and the signal measured by the strain gauges (pitch and plunge displacements) were acquired in time domain using the dSPACE system.

In Fig. 5, one can observe the results obtained in the identification process. The evolution of pitch and plunge frequencies and damping are shown. It can be seen that flutter occurs at a speed near to 25 *m/s* as observed in previous results. The cloud of points is related to the variation of the identified parameters at each test speed. It is important to remark that the identification process show a good matching of frequencies while the damping tendency is acceptable just for the pitch mode, which is the mode that leads to flutter. The damping results relative to the plunge mode are just a qualitative representation. It was considered in this identification *N=2M*.

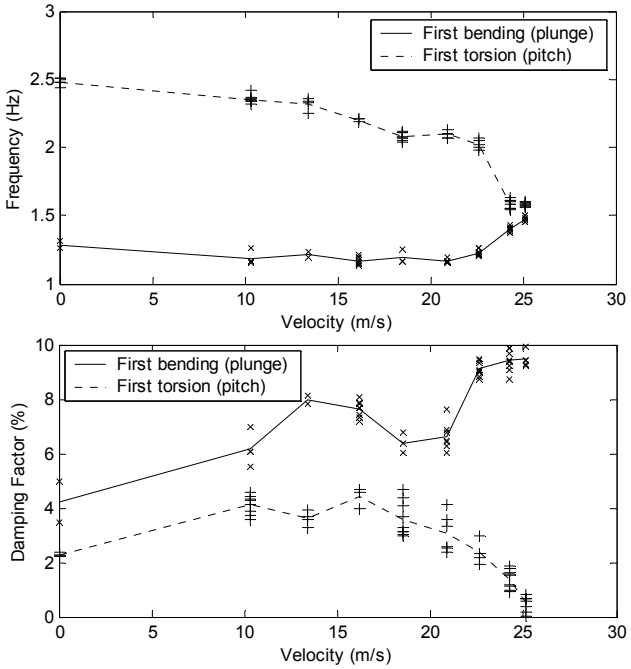

Figure.5 Flutter parameters identified using EERA and data from wind tunnel tests.

6. Conclusions

The experimental system for flutter tests in wind tunnel was successfully developed. Some wind tunnel tests were performed for flutter characterization and the phenomenon could be observed in the time and frequency domain. In the time domain results the self-sustained oscillatory behavior of flutter was observed. In the frequency domain responses the evolution of the modes with wind tunnel increasing velocity was also observed. At the critical velocity, the coupling tendency could be observed. The modifications in pitch and plunge damping could be obtained just in a qualitative way in these tests.

In order to quantify the evolution of pitch and plunge modes with increasing velocity an identification method was applied. The Extended Eigensystem Realization Algorithm was employed using the input and output data obtained, in time domain, during the tests performed for flutter characterization. This method was employed on the identification of flutter parameters in order to verify its performance in terms of velocity and possible numerical problems during the process. Considering these tasks and the coherence of the results obtained this identification method can be said appropriate. Some difficulties occurred in the identification of damping values relative to the plunge mode. But, as can be verified in the results, this is not the most important mode and, consequently, it is not as well defined as the mode that leads to flutter, the pitch one.

Even considering that the identification process performed in this work is an off-line one, the results obtained until now indicate that the objective of this project, the on-line identification of flutter parameters during wind tunnel tests, can be explored. The main objective can be defined as the development of an adaptive control system obtained with the association of the on-line identification method and a control law for flutter suppression.

7. Acknowledgements

The authors gratefully acknowledge the financial support provided by CAPES and FAPESP (São Paulo State Foundation for Research Support – Brazil) through contract numbers 1999/04980-0 and 2000/00390-3.

8. References

Ashley, H., 1970, “Aeroelasticity”, Applied Mechanics Reviews, pp.119-129.

Collar, A.R., 1959, “Aeroelasticity – Retrospect and Prospect”, The Journal of the Royal Aeronautical Society, Vol. 63, No. 577, pp.1-15, 1959.

Dansberry, B.E., Durham, M. H., Bennett, R. M., Turnock, D. L., Silva, E. A. and Rivera Jr, J. A., 1993, “Physical Properties of the Benchmark Models Program Supercritical Wing”, NASA TM-4457.

De Marqui Jr., C., Belo, E.M., Tsunaki, R.H., Rebolho, D.C. and Marques, F.D., 2004, “Design and Tests of an Experimental Flutter Mount System”, Proceedings of the XXII IMAC, Dearborn, MI.

Favoreel, W., Huffel, S.V., De Moor, B, Sima, V. and Verhaegen, M., 1999, “Comparative study between three subspace identification algorithms”, Proceedings of the European Control Conference, Karlsruhe-Germany, 31st August-3rd September, 6p.

Försching, H., 1997, “Aeroelastic Problems in Aircraft Desing”, von Karman Institute for Fluid Dynamics, Lecture series 08: A Survey of Aeroelastic Problems.
Fung, Y.C., 1993, “An introduction to the theory of aeroelasticity”, John Wiley & Sons Inc, United States, 490p.
Garrick, I.E. and Reed, W.H., 1981, “Historical Development of Aircraft Flutter”, Journal of Aircraft, Vol.18, No. 11, pp. 897-912.
Garrick, I.E., 1976, “Aeroelasticity – frontiers and beyond”, 13th Von Karman Lecture, J. of Aircraft, Vol.13, No. 9, pp. 641-657.
Ko, J., Kurdila, A.J. and Strganac, T.J., 1997, “Adaptive Feedback Linearization for the Control of a Typical Wing Section with Structural Nonlinearity”, ASME International Mechanical Engineering Congress and Exposition, Dallas, Texas.
Mukhopadhyay, V., 1995, “Flutter suppression control law design and testing for the active flexible wing”, Journal of Aircraft, Vol.32, No. 1, pp 45-51.
Tasker, F., Bosse, A. and Fisher, S., 1998, “Real-time modal parameters estimation using subspace methods: Theory. Mechanical Systems and Signal Processing”, Vol.12, No. 6, pp. 797-808.
Tsunaki, R. H., 1999, “Identificação Automatizada de Modelos Dinâmicos no Espaço de Estados”, Ph.D. Thesis, University of Sao Paulo.
Verhaegen, M. and Dewilde, P., 1992, “Subspace model identification part 1. The output-error state space model identification class of algorithms”, International Journal of Control, Vol. 56, pp. 1187-1210.
Waszak, M.R., 1998, “Modeling the benchmark active control technology wind-tunnel model for active control design applications”, NASA TP-1998-206270.
Wright, J.R., 1991, “Introduction to Flutter of Winged Aircraft”, von Karman Institute for Fluid Dynamics, Lecture series 01: Elementary Flutter Analysis.

9. Responsibility notice

The authors are the only responsible for the printed material included in this paper.